Design of a Microstrip-based Wideband Wearable Antenna for the 2 to 3 GHz Band

Ezzaty Faridah Nor Mohd Hussin[1], Ping Jack Soh[1*], Mohd Faizal Jamlos[2], Herwansyah Lago[3], Azremi Abdullah Al-Hadi[1], Qassim Abdullahi[4], Dimitris E. Anagnostou[4], Symon K. Podilchak[4*]

[1]Advanced Communication Engineering (ACE) Centre of Excellence, School of Computer and Communication Engineering, Universiti Malaysia Perlis, Perlis, Malaysia

[2]Faculty of Mechanical Engineering, Universiti Malaysia Pahang, 26600, Pekan, Malaysia

[3]Faculty of Engineering, Universiti Malaysia Sabah, 88400 Kota Kinabalu, Sabah, Malaysia

[4]Institute of Sensors, Signals and Systems (ISSS), Heriot Watt University, Edinburgh EH14 4AS, United Kingdom

*Emails: *pjsoh@unimap.edu.my; s.podilchak@hw.ac.uk*

***Abstract*—The design procedure for a wideband wearable antenna made fully using textiles based on microstrip topology is presented. The antenna operates within the 2 to 3 GHz band with a fractional bandwidth of 51 % and low back radiation towards the body. The existence of the ground plane ensures minimal interference with human tissues when worn while it reduces the electromagnetic power that is potentially absorbed into the human tissue. The narrowband characteristics of the antenna are alleviated by integrating several broadbanding techniques: multi-resonance overlapping, increased substrate thickness, added slots and parasitic patches, and finally, impedance tuning using a staircase-like structure. The levels of forward and back radiation are assessed and the antenna features 17 dB front-to-back ratio and 3.5 dBi average gain throughout its operating band.**

***Index Terms*— broadbanding technique, textile antennas, wearable antennas, wideband antenans.**

I. INTRODUCTION

Microstrip antennas are widely used in a multitude wireless communication applications. However, their traditionally narrow bandwidth [1] may hinder their adoption for practical wideband applications of wearable electronics. The introduction of multiple wireless standards throughout the band between 2 and 3 GHz has intensified the research into providing a single antenna hardware to cover operation within this band. Such features translate into space and cost efficiency to operate within popular 2 to 3 GHz bands such as the Wireless Local Area Network (WLAN), Wireless Body Area Network (WBAN) and Long Term Evolution (LTE) bands [2-3]. Besides that, the development of wearable devices with flexible substrates that operate in these bands is of interest because the traditionally rigid substrates of the antennas make current models uncomfortable to the user.

Wideband antennas are typically designed based on the conventional monopole topology. Such an antenna type either requires a partial ground plane or integrated coplanar waveguide structures, which then results in the placement of their ground planes on the same plane as the radiating elements [4-6]. The absence of the full ground plane which acts as a shielding between the antenna and the human body typically results in performance variation and potentially high electromagnetic absorption into human tissue. Several wideband wearable antennas have been proposed and validated for on-body application [7-9]. They include the planar inverted-F antenna (PIFA) which bandwidth was broadened using slots and slits [7], an ultrawideband (UWB) microstrip patch antenna was enabled using a multitude of broadbanding techniques [8], and a wideband planar antenna integrated with a T-shaped slot for the same purpose was achieved in [9].

This work presents the design of a wideband antenna based on the microstrip topology, which operates between 2 and 3 GHz. Fabricated fully using textiles, this antenna was first investigated as a preliminary work via simulations [10] and was integrated with an Artificial Magnetic Conductor (AMC) plane backing in [11]. However, this structure is newly reported due to its better performance when implemented with the full rear ground plane instead of the AMC backing. This is evident when observing the back radiation towards the human user more effectively over the operating band, defined by its front-to-back (FBR) ratio. Such reduction also effectively minimizes electromagnetic absorption in the human tissue, defined in terms of Specific Absorption Rate (SAR).

II. ANTENNA DESIGN AND MATERIALS

A. Textiles

Two textile materials were used in the design of the antenna. First, a felt textile as the antenna substrate, and second the ShieldIt Super™ textile forms the conductive elements. The felt textile is 3 mm thick, and features a relative permittivity of $\varepsilon_r = 1.44$ and loss tangent of $tan\delta = 0.044$. ShieldIt™ is 0.17 mm thick and has conductivity $\sigma = 1.18 \cdot 10^5$ S/m. The reverse side of ShieldIt is supplemented by an adhesive to facilitate its attachment onto the felt substrate. The ShieldIt substrate is fed using a conventional 50 Ω SMA connector.

B. Antenna Design

To support the multi-standard operation using a single radiator structure, the proposed narrowband microstrip antenna incorporates several broadbanding techniques. These include: increasing substrate thickness, overlapping multiple resonances [12], the addition of slots [9], parasitic patches [13-14], and staircase-like structures [15]. To implement these, two layers of felt substrate are used instead of one, resulting in 6 mm overall thickness. Then, a multi-resonance overlapping technique is implemented by introducing two sub-radiators in the form of rectangular patches. These two sub-radiators are designed with different dimensions to operate at different frequencies prior to their integration with each other. The top patch illustrated in Fig. 1 is designed for operation at 1.5 GHz, whereas the other (lower) patch operates at 2.5 GHz. Next, their operation is combined using a microstrip transmission line that connects these two sub-radiators to function as a single radiator. The resulting mismatch in impedance is initially alleviated using step transitions before being further optimized.

To further extend the bandwidth, several slots and slits are then integrated one after another onto the two patches. Two E-shaped slots are first integrated onto the top patch, followed by the incorporation of an F-shaped slit onto the bottom patch. The addition of these slots created a significant size reduction of the combined radiator. Next, a parasitic radiator was introduced and was placed near the two sub-radiators.

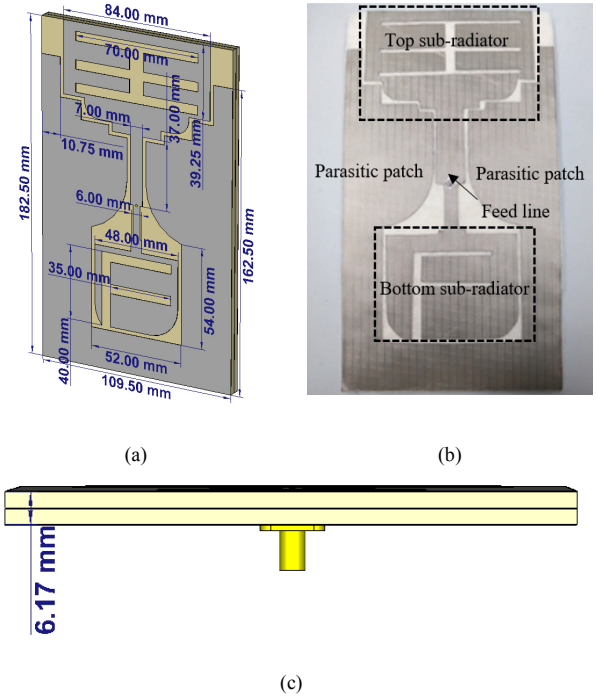

(a) (b)

(c)

Fig. 1. Dimension of the proposed antenna (a) top view simulated; (b) top view fabricated; and (c) side view. Dimensions: $a = 8$, $b = 27$, $c = 13$, and $G = 2$. All dimensions are in mm.

The coupling between the newly introduced parasitic patches and the two sub-radiators increased the bandwidth further. To again match the impedance detuning resulting from the implementation of these bandwidth broadening techniques, steps and blends are then applied onto the radiating and parasitic patches. Finally, the impedance matching for the proposed antenna is further optimized using these slots and slits to ensure that the reflection coefficient across the whole targeted band is less than -10 dB. This impedance tuning process is mainly performed using parametric study.

III. Results and Discussion

A. Parameter Optimization

Optimization of the parameters of the proposed antenna were first performed. This process identified three main design parameters. First is the width of the feed line to the upper patch (*Fw*), secondly, the length of the stepped notch feeding the lower patch (*t*), and finally, the minimum gap between the radiating and parasitic patches (*G*). The optimization of each parameter is performed independently and keeping the rest of the parameter fixed in their values. The variation of each parameter changes in terms of reflection coefficient is summarized in Table 1. It is observed that the changes to *Fw* affected the performance of the antenna in the upper frequency. An optimal line width value of 13 mm is obtained, which resulted in a 45% of fractional bandwidth. Meanwhile, for the second parameter, the length of the stepped notch (*t*) is chosen as 2 mm, which broadened the bandwidth to 1.05 GHz (42.17 %). The largest fractional bandwidth of 43.07 % was produced with $G = 1$ mm. However, this dimension is not selected to avoid fabrication inaccuracy. Instead, a 3 mm gap is used at the cost of a slightly narrower fractional bandwidth of 41.44 %.

B. On Body Performance Evaluation

The next validation for the proposed wearable antenna is to assess its performance when operated on body. This is done using simulations and measurements when the antenna is placed at a distance of 10 mm over the upper arm using a foam-based spacer. In simulations a truncated model of a voxel upper arm with the antenna placed at the same distance and bent using a bending radius of $r = 60$ mm. The use of the

TABLE I. Summary of Antenna Performance Evaluated under Planar and Flexed Conditions

Param.	Condition		
	Planar (FS)	***Bent with r = 60 mm (x-axis)***	***Bent with r = 60 mm (y-axis)***
Sim FBR (dB)	17.74	9.52	14.02
Meas. FBR (dB)	21.09	12.88	18.92
Sim. BW (GHz)	1.05	1.04	1.10
Meas. BW (GHz)	1.30	1.30	1.26
Sim. SAR (W/kg)	N/A	0.111	0.06

truncated voxel model is to ensure reduction of computational resources, whereas measurements were performed when the antenna is placed at the same distance on the upper arm of a human volunteer. Each measurements were performed five times, and the results are averaged and compared with simulations in Table 1. The simulated and measured reflection coefficients (S_{11}) are also illustrated in Fig. 2.

When bent at the *x*-axis, the simulated S_{11} of the antenna indicated a slight decrease in bandwidth to 1.04 GHz. In comparison, the simulated bandwidth in planar form produced a bandwidth of 1.05 GHz. On the contrary, there is a slight increase of the bandwidth to 1.095 GHz when bent at the *y*-axis. The measured antenna bandwidth indicated very small changes when bent at the *x*-axis, relative to the 1.3 GHz bandwidth produced when assessed in free space.

When bent at the *x*-axis, simulated S_{11} of the antenna indicated a slight decrease in bandwidth to 1.04 GHz. In comparison, simulations in planar form produced a bandwidth of 1.05 GHz. On the contrary, there is a slight bandwidth increase to 1.095 GHz when bent at the *y*-axis

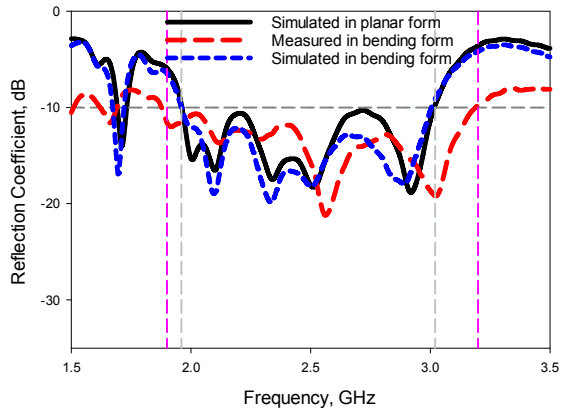

(a)

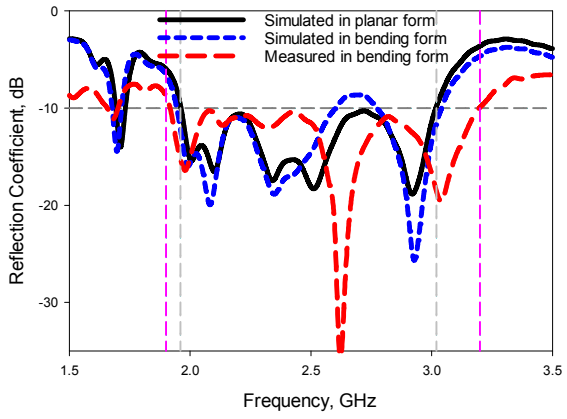

(b)

Fig. 2. Simulated and measured antenna reflection coefficient in free space, planar and bent conditions, when bent at the (a) *x*-axis and (b) *y*-axis.

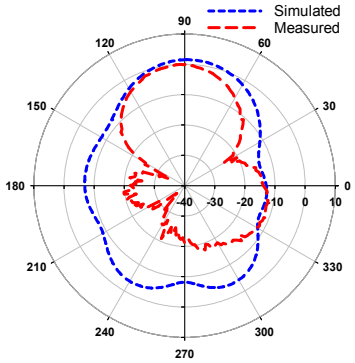

(a)

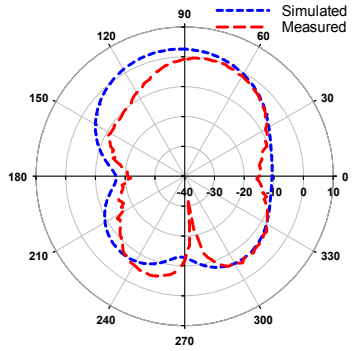

(b)

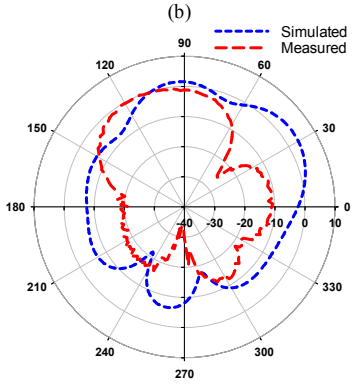

(c)

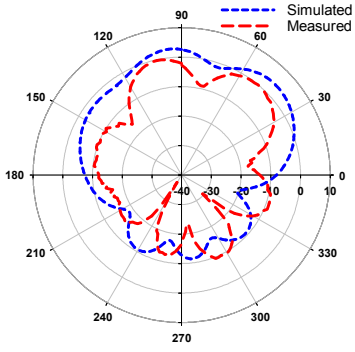

(d)

Fig. 7. Simulated and measured antenna radiation patterns (a) at the *xz*-plane (bent at the *x*-axis), (b) at the *xz*-plane (bent at the *y*-axis), (c) at the *yz*-plane (bent at the *x*-axis) and (d) at the *yz*-plane (bent at the *y*-axis).

Fig. 3.

Fig. 4.

The measured antenna bandwidth indicated very small changes when bent at the *x*-axis, relative to the 1.3 GHz bandwidth produced when assessed in free space. The antenna bandwidth decreased slightly to 1.26 GHz when bent with r = 60 mm at the *y*-axis. These results indicate the robustness of the antenna when used in bent conditions.

The levels of back radiation was reduced due to the proposed microstrip-based structure. This was evaluated in terms of FBR, which is 17.74 dB in simulations and 21.09 dB from measurements when assessed for planar conditions. When bent at the *x*-axis, the simulated FBR of the antenna is reduced to 9.52 dB, whereas bending under *y*-axis resulted in a smaller decrease of the FBR to 14.02 dB. On the other hand, measurements of the antenna's FBR when bent at the *x*-axis also decreased its FBR to 12.88 dB. An interesting behaviour is that the measured FBR when the antenna is bent at the *y*-axis is slightly increased to 18.92 dB. This could be due to the small expected changes in FBR, as was found in simulations, coupled with possible small measurement errors due to the signal fluctuations when calculating the FBR for this bending condition. The simulated and measured radiation patterns are presented in Fig. 3.

The safety level assessment of the proposed antenna for its on-body operation is performed as the final assessment, in terms of SAR. This is assessed based on the regulatory standard provided by [16], with a maximum limit of 2 W/kg, averaged over 10 g of tissue. Simulations were performed using an input power of 0.5 W (rms) with bent antennas placed at 10 mm on the same voxel upper arm model. Due to the unavailability of measurement equipment, the SAR of the proposed antenna was not validated experimentally. The results of the on-body evaluations in terms of bandwidth, FBR, and SAR at 2.45 GHz are also provided in Table 1.

IV. Conclusion

A wideband antenna made fully using textile materials with low back radiation resulting from the use of the microstrip topology is presented and studied. The wideband behaviour of the planar radiator was enabled by using a combination of bandwidth broadening methods such as increasing substrate thickness, multi-resonance overlapping, slots and slits and parasitic patches. This resulted in its operation in the band between 2 GHz and 3 GHz, with a simulated and measured bandwidth 42% and 51%, respectively. Satisfactory levels of antenna gain for wearable applications are also validated, with 4.1 dB obtained from simulations and 3.5 dB from measurements. Evaluations of the antenna under different bending configurations in free space and on the body generally indicated slight degradations in terms of bandwidth and FBR. This is due to the ground plane backing on its rear, which minimized the potential coupling between the radiator and the human body, besides reduced backward radiation. Assessments made numerically and experimentally also validated that the proposed antenna is more suitable to be used on body. Also, the SAR values of the antenna indicated levels lower than the 2 W/kg regulatory limit. Most importantly, this antenna has been validated to be safe and suitable for simultaneous wearable WBAN, WLAN and LTE applications.

Acknowledgment

This project was supported by the Malaysia Ministry of Education under the Fundamental Research Grant Scheme (FRGS) (grant no: FRGS/1/2015/ICT05/UNIMAP/02/2) and the MyBrain15 Scholarship.

References

[1] P. B. Samal, P. J. Soh, and G. A. E. Vandenbosch, "A systematic design procedure for microstrip-based unidirectional UWB antennas," *Progress in Electromagnetics Research*, vol. 143, pp. 105-130, 2013.

[2] A. Alomainy, Y. Hao, C. G. Parini and P. S. Hall, "Comparison between two different antennas for UWB on-body propagation measurements," *IEEE Antennas and Wireless Propagat. Lett.*, vol. 4, no. , pp. 31-34, 2005

[3] H. G. Schantz, "Introduction to ultra-wideband antennas," *IEEE Conf. on Ultra Wideband Systems and Technologies*, 2003, pp. 1-9.

[4] J. Bai, S. Shi, and D. W. Prather, "Modified compact antipodal vivaldi antenna for 4–50-GHz UWB application," *IEEE Trans. Microw. Theory Tech.*, vol. 59, no. 4, pp. 1051–1057, Apr. 2011.

[5] Mandal, T. and Das, S., "Design and analysis of a coplanar waveguide fed ultrawideband hexagonal open slot antenna with WLAN and WiMAX band rejection," *Microw. Opt. Technol. Lett.*, vol. 56, no. 2, pp. 434-443, 2014.

[6] P. J. Soh, G. A. E. Vandenbosch and J. Higuera-Oro, "Design and evaluation of flexible CPW-fed Ultra Wideband (UWB) textile antennas," *2011 IEEE Int. RF & Microwave Conf.*, Seremban, Malaysia, 2011, pp. 133-136.

[7] P. B. Samal, P. J. Soh and G. A. E. Vandenbosch, "UWB All-Textile Antenna With Full Ground Plane for Off-Body WBAN Communications," *IEEE Trans. Antennas Propag.*, vol. 62, no. 1, pp. 102-108, Jan. 2014.

[8] P.J. Soh, G.A. Vandenbosch, S.L. Ooi, and N.H.M. Rais,"Design of a broadband all-textile slotted PIFA," *IEEE Trans. Antennas Propag.*, vol. 60, no. 1, pp.379-384, 2012.

[9] A. Sabban, "New Wideband Compact Wearable Slot Antennas for Medical and Sport Sensors," *Journal of Sensor Technology*, vol. 8, no. 01, pp.18-34, 2018.

[10] E. F. N. M. Hussin, P. J. Soh, M. F. Jamlos, H. Lago and A. A. Al-Hadi, "Wideband textile antenna with low back radiation for wearable applications," *2016 URSI Asia-Pacific Radio Science Conf. (URSI AP-RASC)*, Seoul, Korea, 2016, pp. 1089-1092.

[11] E. F. N. M. Hussin, P. J. Soh, M. F. Jamlos, H. Lago, A. A. Al-Hadi, M. H. F. Rahiman, "A Wideband Textile Antenna with Ring Slotted AMC Plane," *Applied Physics A: Materials Science & Processing*, vol. 123, no. 46, pp. 1 – 7, Jan. 2017.

[12] A. A. Abdelaziz, "Bandwidth enhancement of microstrip antenna," *Progress in Electromagnetics Research*, vol. 63, pp. 311–317, 2006.

[13] M. Koohestani and M. Golpour, "U-shaped microstrip patch antenna with novel parasitic tuning stubs for ultra wideband applications," *IET Microw., Antennas, Propag.*, vol. 4, no. 7, pp. 938–946, Jul. 2010.

[14] W.-C. Liu, C.-M.Wu, and Y.-J. Tseng, "Parasitically loaded CPW-fed monopole antenna for broadband operation," *IEEE Trans. Antennas Propag.*, vol. 59, no. 6, pp. 2415–2419, June 2011.

[15] Kang, D. , Tak, J. and Choi, J., "Low-profile dipole antenna with parasitic elements for WBAN applications," *Microw. Opt. Technol. Lett.*, vol. 58, no. 5, pp. 1093-1097, 2016.

[16] IEC/IEEE 62704 Standard, "Determining the peak spatial-average specific absorption rate (SAR) in the human body from wireless communication devices, 30 MHz to 6 GHz," 1st ed., Oct. 2017.